Dynamic PEG-PLA/hydroxyurethane networks based on imine bonds as reprocessable elastomeric biomaterials

Mathilde Grosjean, Dimitri Berne, Sylvain Caillol, Vincent Ladmiral, Benjamin Nottelet

Dynamic PEG-PLA/hydroxyurethane networks based on imine bonds as reprocessable elastomeric biomaterials

Mathilde Grosjean[a]ǂ, Dimitri Berne[b]ǂ, Sylvain Caillol[b], Vincent Ladmiral[b]*, Benjamin Nottelet[a]*

[a] *IBMM, Univ Montpellier, CNRS, ENSCM, Montpellier, France*

[b] *ICGM, Univ Montpellier, CNRS, ENSCM, Montpellier, France*

ǂ authors contributed equally to this paper

** corresponding authors: B.N. benjamin.nottelet@umontpellier.fr; V.L vincent.ladmiral@enscm.fr*

Abstract

The development of dynamic covalent chemistry opens the way to the design of materials able to be reprocessed by internal exchange reaction under thermal stimulus. Imine exchange differs from other exchange reactions by its relative low temperature of activation. In this study, amine-functionalized star-shaped PEG-PLA and aldehyde-functionalized hydroxyurethane modifier were combined to produce PEG-PLA/hydroxyurethane networks incorporating imine bonds. The thermal and mechanical properties of these new materials were evaluated as a function of the initial ratio of amine/aldehyde used during synthesis. Rheological analyses highlighted the dynamic behaviour of these vitrimers at moderate temperature (60-85 °C) and provided the flow activation energies. Additionally, the reprocessability of these PEG-PLA/hydroxyurethane vitrimers were assessed by comparing the material properties before reshaping and after three reprocessing cycles (1 ton, 1 h, 70 °C). Hence, these materials can easily be designed to satisfy a specific medical application without properties loss. This work opens the way to the development of a new generation of dynamic materials combining degradable PEG-PLA copolymers and hydroxyurethane modifiers, which could find application to shape medical devices on-demand under mild conditions.

Keywords: vitrimer, imine exchange, hydroxyurethane modifier, PEG-PLA

1. INTRODUCTION

Imine functions, also known as "Schiff base", have been discovered by Hugo Schiff in 1864[1] and have been employed as synthetic intermediates or in coordination chemistry.[2,3] Imine bonds are generally synthesized by condensation between an aldehyde or a ketone and a primary amine.[4] Additionally, the reaction can revert to the aldehyde/ketone and amine in the presence of water or under acidic conditions. This reversible exchange (Scheme 1A) occurs according to a dissociative mechanism and has been used in the development of dynamic covalent chemistry.[5,6] In addition to this dissociative mechanism, imine functions can also exchange *via* two associative pathways: transimination (Scheme 1B) and imine metathesis (Scheme 1C).[7,8] These two reactions can take place in the absence of water, under thermal stimulus and without the use of any catalyst.[9] However, transimination requires free primary amines in the system. The exchange proceeds through the formation of a tetrahedral intermediate (aminal) that is subsequently decomposed to form a new imine and amine.[10] Imine metathesis corresponds to the exchange between two imines functions. Although it is accepted in the literature that this exchange takes place by association, the details of the mechanism are still much debated and depend on the catalyst used.[10]

While the potential of imine bonds to undergo thermally driven exchange has been initially exploited in organic chemistry, the incorporation of such bonds in crosslinked networks allows the preparation of a large range of vitrimers.[11–13] Vitrimers exhibit properties inherent to thermosets, including high mechanical properties and solvent resistance, in association with the capability to be reprocessed generally associated to thermoplastics. Multiple reviews have listed the different exchange reactions used in vitrimer materials.[14–19] Among those reactions, imine exchange is valuable due to the high exchange rate observed at moderate temperature.[7] Therefore, transimination and imine metathesis have been used for the development of several dynamic networks such as vanillin- or lignin-based polymers[20–22] but also in chitosan-based hydrogels,[23–27] even if for the latter the term vitrimer was not employed and the characteristic properties of vitrimer materials were not evaluated in details.[28]

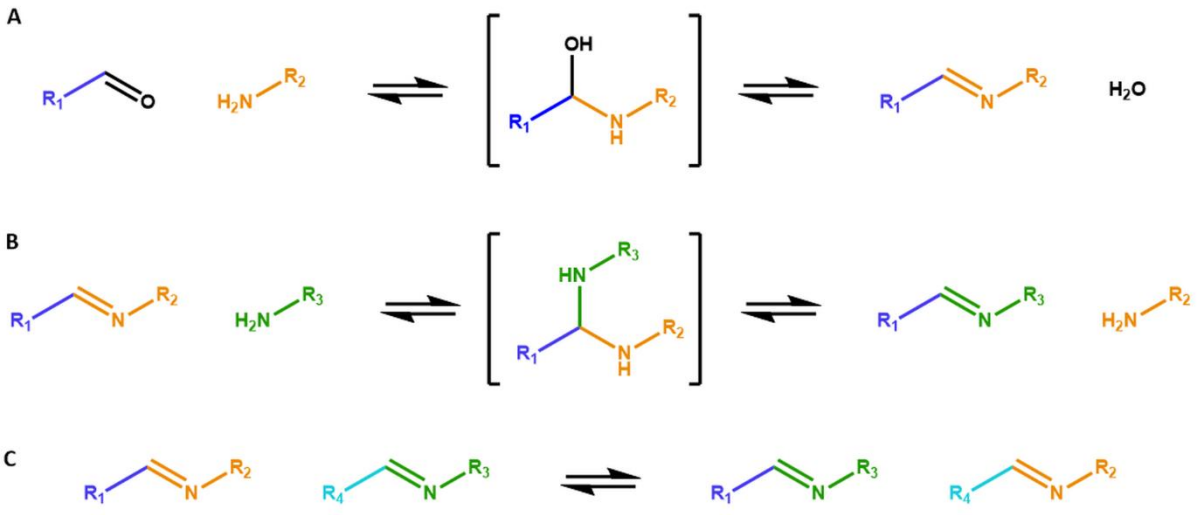

Scheme 1. A. Imine condensation/hydrolysis equilibrium. B. Transimination of an imine with a free primary amine. C. Imine metathesis between two imine functions.

In the context of the development of sustainable networks, the replacement of isocyanates in the synthesis of urethanes is a crucial challenge. Indeed, urethanes generally result from the reaction of alcohols and isocyanates. Most of isocyanate reactants are known to be harmful for human health and for the environment[29,30] and need to be replaced in a near future. Hydroxyurethanes can be obtained by the aminolysis of 5-membered cyclic carbonates which is arguably the most promising synthesis route to isocyanate-free urethanes NIPU.[31–33] Indeed, the 5-cyclic carbonates required to perform this synthesis can be prepared through the carbonation of epoxy functions by CO_2, which is a cheap, renewable and non-toxic resource.[34–36] Nevertheless, some remaining challenges regarding the use of hydroxyurethanes slow down the industrial development of poly(hydroxyurethanes) (PHUs).[31] The presence of hydroxyl group limits the kinetics, degree of advancement of the carbonate aminolysis and the molar mass of the PHUs. The PHUs thus do not possess identical properties to their polyurethane equivalents.[37,38] However, the use of hydroxyurethane modifiers (HUM) pioneered by Figovsky et al. is of high interest to improve the properties of other polymers in a sustainable approach.[39,40] The hydroxyl functions are nonetheless interesting to further chemically modify PHUs with different functions and thus extend their application range.

This study proposes new hybrid (combination of ether, ester and urethane functions) vitrimer materials based on imine exchange and incorporating urethane, ethylene glycol and lactic acid units. We chose

to associate hydroxyurethanes to biocompatible copolymers of bioeliminable poly(ethylene glycol) (PEG) and biodegradable poly(lactic acid) (PLA) to expand the application range of hydroxyurethane materials to the biomedical field and develop a vitrimer system suitable to biomedical applications. A di-hydroxyurethane modifier was synthesized from a di-cyclic carbonate and then esterified using 4-formylbenzoic acid to yield an aldehyde functional urethane modifier. In parallel, an 8-arm star PEG-*b*-PLA block copolymer was synthesized *via* ring opening polymerization and the chain-ends were functionalized with amine moieties. These two components were then combined to form crosslinked networks *via* the condensation of amine and aldehyde moieties into reversible imine bonds thus conferring dynamic properties to the materials. Chemical and physical properties of this novel networks were first evaluated to highlight the combination of urethane units and PLA. Then, an in-depth rheological evaluation of the dynamic properties of the new vitrimer materials was carried out. Finally, the reprocessability of imine vitrimers in mild conditions (1 ton, 1 h, 70 °C) was assessed through multiple characterizations, including gel fraction measurements, thermal analyses and mechanical properties evaluation.

2. MATERIALS AND METHODS

2.1. Materials

D,L-lactide was purchased from Corbion (Gorinchem, The Netherlands). Hydroxyl-terminated eight-arm poly(ethylene glycol) (tripentaerythritol) (PEG_{8arm}10k, Mw = 10,000 $g.mol^{-1}$) was purchased from JenKem Technology Co., Ltd (Beijing, China). Tin(II) 2-ethylhexanoate (Sn(Oct)2), dichloromethane (DCM), ethanol (EtOH), tetrahydrofuran (THF), ethyl acetate (AcOEt), methanol (MeOH), N,N'-dicyclohexylcarbodiimide (DCC), 4-dimethylaminopyridine (DMAP), 4-aminobenzoic acid, 4-formylbenzoic acid, Celite ® 545, 1,4-butanediol diglycidyl ether (BDGE), tetrabutylammonium bromide (TBAB), ethanolamine and benzophenone were purchased from Sigma-Aldrich (St Quentin Fallavier, France).

2.2. Methods

2.2.1. Size exclusion chromatography

Average molecular weights ($\overline{Mn}$) and dispersities (Đ) were determined by size exclusion chromatography (SEC, Shimadzu SIL-20A HT) using two mixed medium columns PLgel 5 µm MIXED-C (300 x 7.8 mm), a Shimadzu RI detector 20-A and a Shimadzu UV detector SPD-20A (260 and 290 nm) (40°C thermostatic analysis cells). THF was the mobile phase eluting at 1 $mL.min^{-1}$ flow at 30°C (column temperature). Polymers were dissolved in THF to reach a concentration of 5 $mg.mL^{-1}$. The solutions were filtered through a 0.45-µm Millipore filter before injection. $\overline{Mn}$ and Đ were expressed according to calibration using polystyrene narrow standards.

2.2.2. Nuclear magnetic resonance

Nuclear Magnetic Resonance (NMR) (^{1}H and ^{13}C NMR) experiments were carried out in deuterated solvents using a Bruker Avance III 400 MHz NMR spectrometer at 25 °C.

^{1}H 2D diffusion-ordered (DOSY) NMR spectra were recorded on a Bruker Avance III 600 MHz (Bruker, Fällanden, Switzerland) spectrometer equipped with a 5-mm TCI Prodigy Z-gradient cryoprobe. The standard gradient amplifier (GREAT 1/10-E) generates a maximum gradient strength of 65.7 Gauss cm^{-1} at a current of 10 A. The gradient strengths were calibrated using a sample of D2O 99.96 % deuterated from Eurisotop (Saint-Aubin, France). Diffusion measurement was performed with double stimulated echo and bipolar gradient pulses for convection compensation and Eddy current delay (dstebpgp) in a pseudo 2D mode and processed with the Bruker software T1/T2 package from Topspin3.6.2 (Bruker). For this experiment, 16 dummy scans and 32 scans were used with a relaxation delay of 3 s. Diffusion Time Δ was fixed to 0.3 s and gradient strength δ to 2.8 ms. Sinusoidal shapes were used for the gradients and a linear gradient ramp with 16 increments between 2 and 95 % was applied for the diffusion relevant gradients. The diffusion coefficients were calculated with the Bruker software package T1/T2 from Topspin 3.6.2 (Bruker). All diffusion coefficients were within an error range of ±5 %.

2.2.3.High Resolution Mass Spectroscopy (HRMS)

High Resolution Mass spectroscopy (HR-MS) analyses were recorded on a Bruker Daltonics micrOTOF-Q with an ESI source and a positive ion polarity.

2.2.4.Thermogravimetric analysis

Thermogravimetric analyses (TGA) were carried out using a TG 209F1 apparatus (Netzch). Approximately 10 mg of sample were placed in an aluminium crucible and heated from room temperature to 580 °C at a heating rate of 20 °C min^{-1} under nitrogen atmosphere (60 $mL.min^{-1}$).

2.2.5.Differential scanning calorimetry

Thermal properties of the polymers were analysed by differential scanning calorimetry (DSC) using a Mettler Toledo DSC 3 STAR System instrument. Analyses were carried out under nitrogen atmosphere. Samples were heated from 0°C to 100°C (10°C.min^{-1}), then cooled to -80°C (10°C.min^{-1}), before a second heating ramp to 200°C (5°C.min^{-1}). The glass transition temperature (Tg) was measured on the second heating ramp.

2.2.6. Fourier-transform infrared spectroscopy

Fourier-transform infrared spectroscopy (FTIR) spectra were recorded with a Perkin Elmer Spectrum 100 spectrometer for the comparison of initial and reshaped materials and on a Nicolet 210 spectrometer, equipped with an ATR accessory for the fine characterizations of vitrimer characteristic bands.

2.2.7.Titration of the carbonate, aldehyde and amine equivalent weight by ^{1}H NMR

The Carbonate, Aldehyde and Amine Equivalent Weight (CEW, ALEW and AMEW) is the mass of product corresponding to one equivalent of respectively one reactive carbonate, aldehyde or amine function. The equivalent weight was determined by ^{1}H NMR using benzophenone as an internal standard. Determined amounts of product and benzophenone were weighed and placed into an NMR tube, in which 600 µL of $CDCl_3$ was added. The CEW, ALEW and AMEW were determined using equations (1), (2) and (3), respectively. The integration of the signals assigned to benzophenone

protons (7.5–7.8 ppm) were compared to the signals of cyclic carbonate moiety protons (4.6 ppm), of aldehyde moieties (10.1 ppm) and of the CH protons in β position to the primary amine groups (6.5 ppm) for the respective determination of the CEW, ALEW and AMEW. The measurement of each equivalent weight was performed in triplicate.

$$CEW = \frac{I_{benzophenone} \times H_{carbonate}}{I_{carbonate} \times H_{benzophenone}} \times \frac{m_{carbonate}}{m_{benzophenone}} \times M_{benzophenone} \quad (1)$$

$$ALEW = \frac{I_{benzophenone} \times H_{aldehyde}}{I_{aldehyde} \times H_{benzophenone}} \times \frac{m_{aldehyde}}{m_{benzophenone}} \times M_{benzophenone} \quad (2)$$

$$AMEW = \frac{I_{benzophenone} \times H_{amine}}{I_{amine} \times H_{benzophenone}} \times \frac{m_{amine}}{m_{benzophenone}} \times M_{benzophenone} \quad (3)$$

2.2.8. Swelling index

Three samples from the same material, of around 20 mg each, were separately immersed in DCM for 24 h. The swelling index (SI) was calculated using equation (4), where m_2 is the mass of the swollen material and m_1 is the initial mass. Reported swelling index are average values of the three samples (n=3).

$$SI = \frac{m_2 - m_1}{m_1} \times 100 \quad (4)$$

2.2.9. Gel content

Three samples from the same material, of around 20 mg each, were separately immersed in DCM for 24 h. The samples were then dried in a ventilated oven at 70 °C for 24 h. The gel content (GC) was calculated using equation (5), where m_3 is the mass of the dried material and m_1 is the initial mass. Reported gel content are average values of the three samples (n=3).

$$GC = \frac{m_3}{m_1} \times 100 \quad (5)$$

2.2.10. Tensile tests

Dog-bone strips were stamped from polymer films, and their thickness was measured with a micrometer. The mechanical properties were assessed at room temperature on dog-bone strips (10 x 2 mm) with an Instron 3344 testing machine equipped with a 500 N load cell at a deformation rate of 10 $mm.min^{-1}$. Tensile tests were carried out on 5 specimens and the two extreme values were excluded. Young's modulus (E, MPa), stress at yield (σ_{yield}, MPa), strain at yield (ε_{yield}, %), stress at break (σ_{break}, MPa) and strain at break (ε_{break}, %), were expressed as the mean value of three measurements (n=3).

2.2.11. Dynamic mechanical analysis

Dynamic mechanical analysis (DMA) was carried out on a Mettler Toledo DMA 1 Star System in tensile mode with temperature scans from -60°C to 60°C at a frequency of 1Hz with a fixed strain of 0.1% and a preload of 1N. The heating rate was $2°C.min^{-1}$. Rectangle specimens (10 x 3 mm) were used. The thickness of the films was measured with a micrometer. The storage modulus (E'), the loss modulus (E'') were expressed in MPa, tan δ is dimensionless according to equation (6). Tα was determined as the temperature for which the value of E'' was maximum.

$$\tan \delta = \frac{E'}{E''} \quad (6)$$

2.2.12. Rheology

Rheological experiments were performed on a ThermoScientific Haake Mars 60 rheometer equipped with a lower electrical temperature module, with a textured 8-mm plane-plane geometry. A 0.2 N axial force was applied to ensure proper contact between the plates and the samples. For stress relaxation experiments, a 2 % strain was applied on 8 mm diameter and 1 mm thickness circular samples, and the rubbery modulus evolution with time was monitored at different temperatures. Creep recovery experiments were performed at different isotherms by applying 500 Pa shear stress for a duration of 1200 s followed by a recovery period of 1200 s.

2.2.13. Reprocessing of the materials and self-healing study

The reprocessing behaviour of the materials was examined using a Carver 3960 manual heating press. The samples were cut into pieces before pressed at 70 °C for 1 h under 1 ton, and then cooled to room temperature (ca. 20°C) before removing them from the hot press.

The self-healing was studied visually. The samples were cut into two pieces. Then, the pieces were put together along the cutting line, pressed for 5 s, and heated at 70°C in an oven for 1 h.

2.2.14. Degradation study

Samples were cut (10 mm x 10 mm), weighed (Wi = initial weight), and placed in 10 mL of PBS (pH 7.4) at 37°C under stirring. At different time points, samples were removed from PBS and dried to constant mass (Wx = dry weight after x time in PBS). The remaining mass of the samples was calculated from equation (7). The experiment was run in triplicate.

$$Remaining\ mass\ (\%) = \frac{Wx}{Wi} * 100 \qquad (7)$$

2.3. Synthesis of PEG-PLA prepolymer and hydroxyurethane modifier

2.3.1. PEG_{s8}-PLA-NH_2

PEG_{s8}-PLA

For the sake of clarity, PLA_x corresponds to PD,L-LA (50% of L and D units) with a degree of polymerization DPn = x.

Star-shaped copolymer PEG_{8arm}10k-$(PLA_{69})_8$ (PEG_{s8}-PLA) was synthesized by bulk ring-opening polymerization (ROP) following the protocol described previously.[41]

Amine functional PEG_{s8}-PLA (PEG_{s8}-PLA-NH_2)

The 8-armed star block copolymer PEG_{s8}-PLA was solubilized in DCM (10% w/v). Determined amounts (5 eq./OH group) of DCC, DMAP and 4-aminobenzoic acid were added. The mixture was then heated at 40°C for 4 days under stirring. Then, the reaction medium was filtered on Celite ® 545 before being washed with distilled water and concentrated. Afterwards, the mixture was precipitated in cold EtOH. The phenylamine functional PEG_{8arm}10k-$(PLA_{69})_8$-AM (PEG_{s8}-PLA-AM) was dried under reduced pressure to constant mass.

The functionalization was confirmed by ^{1}H NMR and DOSY-NMR.

The yield of functionalization (90 %) was determined by comparing the integration of the phenylamine characteristic signal at 7.6, 6.5 and 6.1 ppm and the integration of the proton resonance at 3.5 ppm.

^{1}H NMR (400 MHz; DMSO-d_6): δ (ppm) = 7.6 (m, 2H aromatic ring, C=C***H***=CH=C-NH_2), 6.5 (m, 2H aromatic ring, C=CH=C***H***=C-NH_2), 6.1 (s, 2H, C=CH=CH=C-N***H$_2$***), 5.2 (q, 1H, CO-C***H***-(CH_3)-O), 4.2 (m, 2H, O-CH_2-C-C***H$_2$***-O), 3.5 (s, 4H, C***H$_2$***-C***H$_2$***-O), 3.3 (m, 2H, O-C***H$_2$***-C-CH_2-O), 1.5 (t, 3H, CO-CH-(C***H$_3$***)-O) (Figure S1).

2.3.2. Aldehyde functional di-hydroxyurethane modifier

Di-cyclic carbonate

BDGE (20 g, 98.8 mmol) and TBAB (0.3 g, 0.12 mmol) were solubilized in 50 mL of AcOEt and added to a 100 mL sealed reactor. The reaction was carried out at 80 °C under 20 bar of CO_2 for 72 h. The crude mixture was then washed with water and brine to remove TBAB. The organic layer was dried with magnesium sulfate and under vacuum. The pure product was obtained as a white solid (yield = 89 %).

^{1}H NMR (400 MHz; $CDCl_3$): δ (ppm) = 4.8 (m, 2H cyclic carbonate, O-CH_2-C***H***-O), 4.5 (m, 2H cyclic carbonate, O-C***H$_2$***-CH-O), 4.4 (m, 2H cyclic carbonate, O-C***H$_2$***-CH-O), 3.6 (m, 4H, CH-C***H$_2$***-O), 3.5 (m, 4H, O-C***H$_2$***-CH_2), 1.7 (m, 4H, O-CH_2-C***H$_2$***) (Figure S2).

Di-hydroxyurethane modifier (HUM)

The di-cyclic carbonate (3.74 g, 1 carbonate equivalent) was reacted with ethanolamine (1.53 g, 1 amine equivalent) in solvent free-conditions for 4 h at 70 °C. The di-hydroxyurethane modifier (HUM) was obtained as a viscous brown liquid (yield = 98 %).

^{1}H NMR (400 MHz; $CDCl_3$): δ (ppm) = 4.6 (m, O-CH_2-C***H***-CH_2), 3.9 (m, CH-C***H$_2$***-OH), 3.7 (m, C***H***-CH_2-OH), 3.5 (m, O-C***H$_2$***-CH-C***H$_2$***-O), 3.4 (m, O-C***H$_2$***-CH_2 and CH_2-C***H$_2$***-OH), 3.3 (m, O-CH-C***H$_2$***-O), 3.0 (C***H$_2$***-CH_2-OH), 1.5 (m, O-CH_2-C***H$_2$***). (Figure S3).

Aldehyde functional di-hydroxyurethane modifier (HUM-CHO)

HUM was solubilized in THF (10% w/v). Determined amounts (1.5 eq./OH group) of DCC, DMAP and 4-formylbenzoic acid were added. The mixture was then heated at 40°C for 3 days under stirring. Then, the reaction medium was filtered on Celite ® 545 before to be concentrated. Afterwards, the crude product was diluted in EtOAc and purified by flash column chromatography (ethyl acetate/ methanol 95/5 v/v). The resulting HUM-CHO was dried under reduced pressure to constant mass.

The yield of functionalization (95 %) was determined by comparing the integration of the formylbenzoic acid characteristic signal at 10.1 ppm and the integration of the proton resonance at 1.6 ppm.

^{1}H NMR (400 MHz; $CDCl_3$): δ (ppm) = 10.1 (s, C=CH=CH=C***H***O), 8.2 (m, 2H aromatic ring, C=C***H***=CH=CHO), 7.9 (m, 2H aromatic ring, C=CH=C***H***=CHO), 6.3 (m, O-CH_2-C***H***-CH_2), 5.5 (m, CH-C***H$_2$***-O-CO), 5.3 (m, C***H***-CH_2-O-CO), 4.6 (m, O-C***H$_2$***-CH-C***H$_2$***-O), 4.5 (m, O-C***H$_2$***-CH_2 and CH_2-C***H$_2$***-O-CO), 3.6 (m, O-CH-C***H$_2$***-O), 3.4 (C***H$_2$***-CH_2-O-CO), 1.6 (m, O-CH_2-C***H$_2$***) (Figure S4).

HRMS (ESI+): theoretical m/z for $[M-H]^+$: 941.2988, measured: 941.2968.

2.3.3. Preparation of vitrimer materials

The materials were prepared by the solvent evaporation method. PEG_{s8}-PLA-NH_2 and HUM-CHO were first solubilized in DCM (10% w/v) at 1/1 and 1/1.5 aldehyde/amine ratio. Then, the solutions were slowly dried at 25 °C in a mold to obtain films, which were further dried under vacuum for 12 hours at 25 °C. The resulting films were crosslinked under vacuum in an oven at 80°C for 24 hours.

3. RESULTS AND DISCUSSION

3.1. Synthesis of PEG-PLA prepolymer and hydroxyurethane modifier

With the objective to design vitrimers combining the properties inherent to PEG-PLA copolymers - degradability, cytocompatibility, tunable mechanical properties- with the properties of urethane functions –H-bonding capability, material structuration *via* supra-interactions- an 8-arm star PEG-PLA

block copolymer end-functionalized with amine moieties (PEG_{s8}-PLA-NH_2) and a di-hydroxyurethane modifier bearing aldehyde groups (HUM-CHO) were prepared.

Regarding the PEG-PLA copolymer, the star topology was selected as it was demonstrated in several studies that it confers higher mechanical properties compared to linear equivalents.[41–45] Moreover, the star-shape structure guarantees a high functionality and therefore a high efficiency in the preparation of crosslinked networks.[41] The synthesis of PEG_{s8}-PLA-NH_2 proceeded in two steps (Figure 1). First, PEG_{s8}-PLA was synthesized by ROP of lactide from an 8-arm hydroxy-terminated PEG.[41] The molar mass calculated by ^{1}H NMR ($\overline{Mn}_{NMR} = 51{,}400$ g.mol^{-1}) agreed with the targeted one and a low dispersity below 1.2 was confirmed by SEC analysis. Then, the OH-terminated star block copolymer PEG_{s8}-PLA was reacted with 4-aminobenzoic acid to yield the desired amine-functionalized star PEG_{s8}-PLA-NH_2. The experimental molar mass ($\overline{Mn}_{NMR} = 51{,}900$ g.mol^{-1}), the monomodal distribution and the low dispersity (1.2) determined by SEC analysis indicated that no degradation of the copolymer occurred during this step. A typical ^{1}H NMR spectrum of PEG_{s8}-PLA-NH_2 is shown in Figure S1. By comparison between the integration of the signals of the methylene groups of PEG at 3.5 ppm and of the phenylamine chain-ends (at 7.6 and 6.5 ppm), a functionalization degree of 90% was calculated. As shown in Figure S5, the grafting of phenylamine functions was also confirmed by the appearance of the UV signal (280 nm) on SEC analysis. Finally, ^{1}H DOSY NMR spectroscopy experiment further confirmed the success of the functionalization since the signals corresponding to the backbone of the copolymers and of phenylamine had the same coefficient of diffusion (Figure S6). The AMEW of PEG_{s8}-PLA-NH_2 was determined to be 8,264 g/eq.

The synthesis of HUM-CHO was performed in three steps (Figure 1). First, a di-cyclic carbonate was prepared by carboxylation of BDGE at 80 °C under 20 bar of CO_2 (Figure S2). BDGE was used as the epoxy source due to its similarities with PEG, which should favour the formation of a homogenous network. The di-cyclic carbonate CEW was 145 g.eq^{-1} which confirmed a high epoxy conversion and its functionality was estimated to 2.0. Then, this di-cyclic carbonate was reacted with ethanolamine at 70 °C for 4 h to form a HUM. This telechelic modifier was composed of two hydroxyurethane units and was terminated with the hydroxyl functions coming from the ethanolamine reactant. The

conversion of the carbonate functions (4.4 ppm) was confirmed by ^{1}H-NMR (Figure S3). Finally, the different hydroxyl groups present in HUM were esterified with 4-formylbenzoic acid in the presence of DCC/DMAP in THF at 40 °C for 72 h to yield to a (multi)aldehyde modifier with a urethane core HUM-CHO. A typical ^{1}H NMR spectrum of HUM-CHO is shown in Figure S4. By comparison between the integration of the signal of the CH_2 group of the BDGE core and of the benzalaldehyde chain-ends, a functionalization degree of 95% was calculated. Finally, an ALEW of 257 g/eq. was determined for HUM-CHO.

These results confirmed the successful functionalization of the PEG-PLA star polymer and of the urethane modifier with amine and aldehyde moieties, respectively, which will allow the preparation of vitrimers based on imine exchange. Moreover, the high functionality of both components offers the possibility to tune the amine/aldehyde ratio which should impact the properties of the resulting networks.

3.2. Preparation of the vitrimer materials

Crosslinked vitrimer materials were prepared from HUM-(CHO) and PEG_{s8}-PLA-NH_2 via the condensation of aldehyde and amine functions yielding imine bonds (Figure 1).

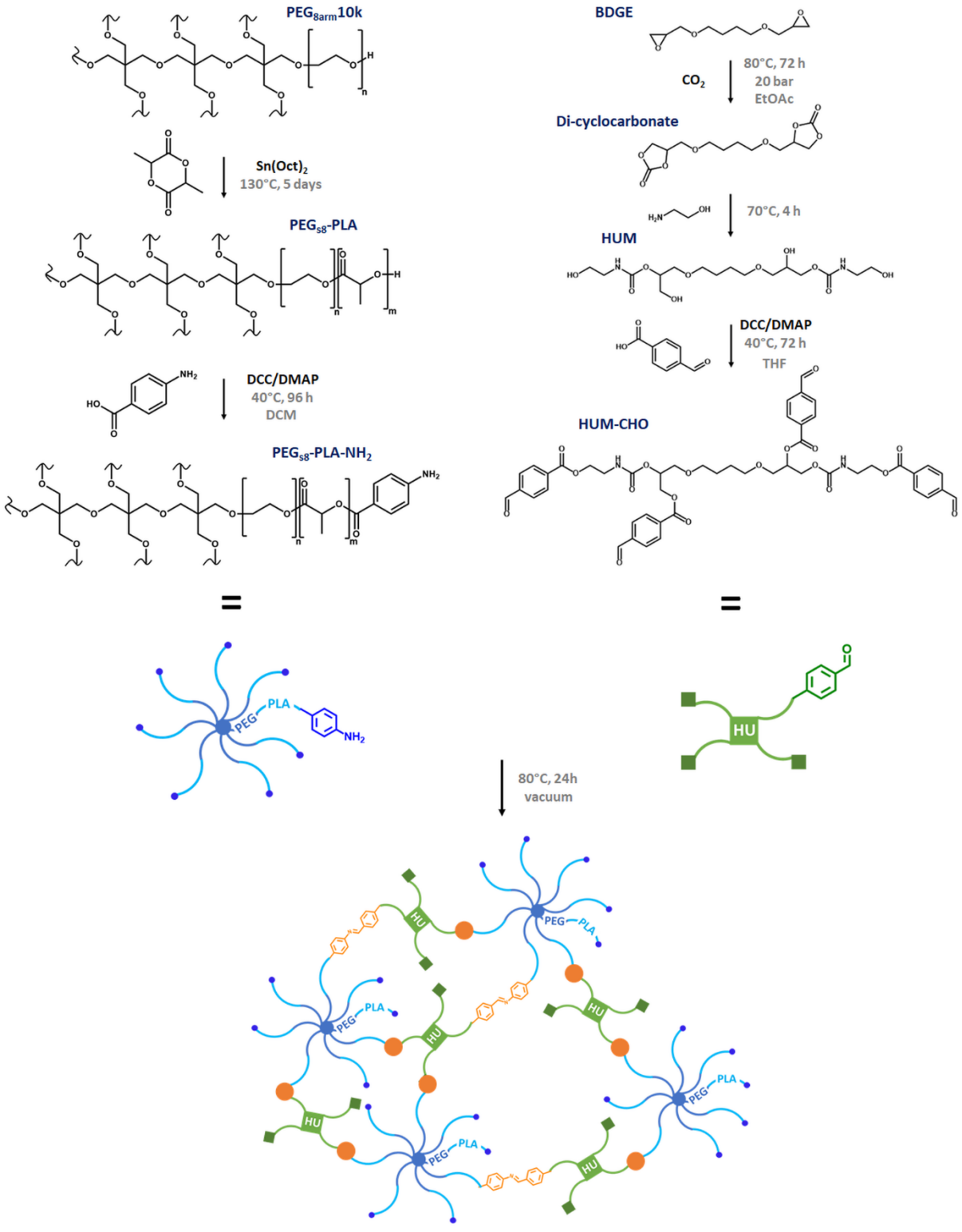

Figure 1. Schematic representation of the formation of the crosslinked networks.

Polymer films were prepared by solvent casting. After solubilisation of the PEG-PLA prepolymer and the HUM-CHO in DCM, these solutions were left to dry overnight at 25 °C into films that were further dried at 25°C under vacuum for 12 h and then cured at 80 °C for 24 h under vacuum. Since the

formation of imine functions from aldehyde and amine is reversible, removal of the water formed during the condensation reaction was necessary to drive the equilibrium towards the formation of imine and thus ensure the formation of a crosslinked network. Undesirable amidation of the PLA chains could be prevented by avoiding a prolonged heating at a temperature above 100°C.[46] TGA analyses of the PEG-PLA-NH_2 prepolymer and the HUM-CHO confirmed that no thermal degradation occurred at this temperature. The protocol described above was used to prepare the imine vitrimers V1 and V1.5 using initial aldehyde/amine ratio of 1:1 and 1:1.5., respectively. Both V1 and V1.5 were yellow and translucent. The yellow coloration is characteristic of the Schiff base formation[47] and is therefore a first indication of the formation of imine bonds as the two initial reactants were colorless.

Table 1. Gel fraction (GC), swelling index (SI), glass transition temperature (Tg), mechanical transition temperature (Ta), and degradation temperature for 5% weight loss ($Td^{5\%}$) of hybrid vitrimers. Data are expressed as the mean ± SD and correspond to measurements with n=3.

Sample	GC (%)[a]	SI (%)[a]	T_g (°C)	T_α (°C)	$T_d^{5\%}$ (°C)
V1	89 ± 2	238 ± 15	20	15	278
V1.5	85 ± 1	272 ± 12	16	13	257

[a]*Gel content and swelling indexes measured after 24 h immersion in DCM at 25 °C.*

First, the network formation was characterized by gel fraction measurements (Table 1). The samples exhibited high gel fractions, with values of 89 ± 2 and 85 ± 1 for V1 and V1.5 respectively, confirming the formation of networks with high crosslinking efficiency. These results are related to the high functionality of the two initial reactants (7.2 for PEG_{s8}-PLA-NH_2 and 3.8 for HUM-(CHO)) used for the formation of the imine vitrimers. As expected, V1.5 displayed a slightly lower gel fraction value due to the presence of free amines in the network. The swelling indexes of the materials in DCM were high due to the relative chain mobility brought by PEG and PLA polymer chains and to the relatively large distance between crosslinking points. V1 demonstrated a slightly lower swelling index than V1.5 directly related to the relative crosslinking density of the two networks.

FTIR analyses were performed on PEG_{S8}-PLA-NH_2, V1 and V1.5 to assess the formation of imine networks (Figure S7). The presence of low intensity C=N stretching band in V1 and V1.5 at 1604 cm^{-1}

confirmed the presence of imine bonds in these two networks.[48] Moreover, bands at 3326 and 1630 cm^{-1} corresponding to N-H stretching and N-H bending, respectively, could be observed in V1.5 and PEG_{S8}-PLA-NH_2 whereas these bands were not visible in V1 spectra. This confirms that V1.5 contains excess amines whereas V1 does not. Finally, the band at 1747 cm^{-1} widened towards lower wavenumbers in V1 and V1.5 compared to PEG_{S8}-PLA-NH_2. This is due to the fact that this band corresponds not only to the stretching of ester C=O bond (as in PEG_{S8}-PLA-NH_2) but also to the stretching of C=O bond associated to the urethane functionalities incorporated in these vitrimers.

After confirming the formation of the network, the thermal properties of the imine vitrimers were investigated. TGA demonstrated that the crosslinked materials were thermally stable up to 250 °C (5 % weight loss) and can therefore be used over a large range of temperature (Figure S8). V1.5 and V1 gravimetric thermograms are similar to the one of PEG_{s8}-PLA-NH_2 . Hence, the thermal stability of the final materials seems mainly dictated by the thermal stability of PEG_{s8}-PLA-NH_2 as it is the major component of the imine vitrimers. DSC analyses were also performed. PEG_{s8}-PLA-NH_2 and HUM-(CHO) displayed glass transition temperatures of 16 and 4 °C (Figure S9), respectively, whereas the T_g of V1 and V1.5 reached 20 and 16 °C respectively (Figure S10). Once again, as PEG_{s8}-PLA-NH_2 is the main component of the final imine vitrimers, it is not surprising to obtain T_g for the final materials relatively close to that of PEG_{s8}-PLA-NH_2. As it was also expected, the excess of amine in V1.5 makes the network looser (lower cross-link density) than for V1 which induced a decrease of the T_g for V1.5 compared to V1. The glass transition temperatures remained relatively low compared to the temperatures needed for imine exchange to occur sufficiently fast.[7,49,50] Hence the glass transition should not impact the observation of materials dynamic properties. The evolution of the mechanical properties of the imine vitrimers as a function of temperature were evaluated *via* DMA (Figure 2). The transition from the glassy to the rubbery state can be also observed with this technique and T_α of 15 and 13 °C were reported for V1 and V1.5, respectively, in agreement with the values and trends of T_g determined *via* DSC. The storage modulus on the glassy plateau was slightly higher for V1 (E' = 3.4 GPa) than for V1.5 (E' = 1.9 GPa) as a result of their respective crosslinking density. No clear rubbery plateau was observed. This is a first demonstration of the fast imine exchange rate upon heating.

Indeed, above 40 °C imine exchanges already occur significantly enough to impact the storage modulus of the materials. Nonetheless, the materials did not flow totally as the storage modulus remained above the loss modulus up to 60 °C.

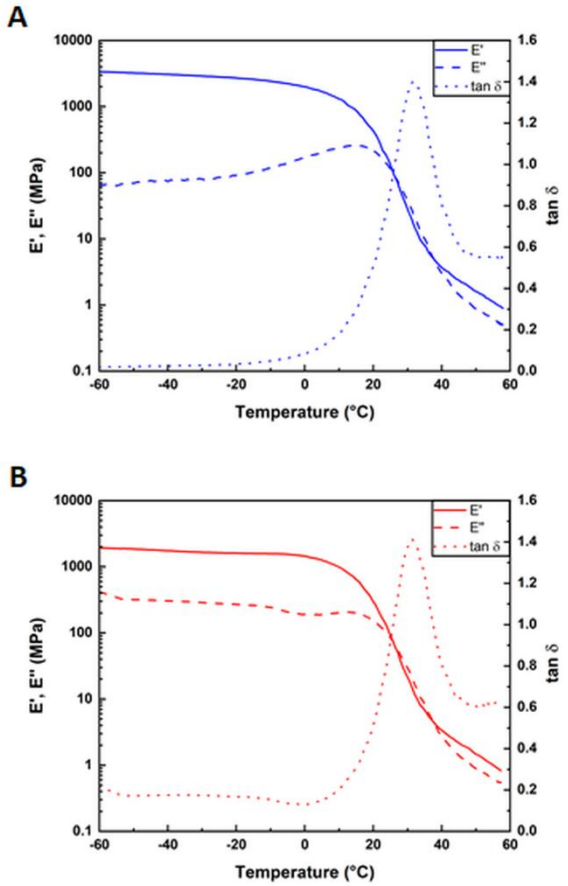

Figure 2. Dynamic mechanical analyses (temperature scan) of hybrid vitrimers with A. V1 and B. V1.5.

The mechanical properties of V1 and V1.5 were assessed through uniaxial tensile tests at room temperature. The results are presented in Table 2.

Table 2. Mechanical properties of the crosslinked networks at room temperature (before and after 3 reshaping). Data are expressed as the mean ± SD of three measurements.

	Number of reshaping	**E (MPa)**	**σ_{yield} (MPa)**	**ε_{yield} (%)**	**σ_{break} (MPa)**	**ε_{break} (%)**
V1	0 – starting material	13.9 ± 2.5	2.1 ± 0.4	10 ± 1	6.7 ± 1.2	596 ± 95

	3	12 ± 1.4	2.2 ± 0.2	11 ± 1	7.2 ± 1.7	719 ± 102
V1.5	0 – starting material	10.7 ± 1.2	1.5 ± 0.2	9 ± 1	4.6 ± 1.8	637 ± 127
	3	11.3 ± 1.5	1.5 ± 0.2	10 ± 1	4.5 ± 1.3	665 ± 121

As expected, the free amines content impacted the mechanical properties (Figure 3). Due to its higher crosslinking density, V1 displayed slightly superior Young's modulus (13.9 ± 2.5 MPa) than V1.5 (10.7 ± 1.2 MPa). Similarly, V1 (σ_{break} = 6.7 ± 1.2 MPa) reached a moderately higher stress at break than V1.5 (σ_{break} = 4.6 ± 1.8 MPa). Moreover, the off-stoichiometry used for V1.5 induces a decrease of the crosslinking density of the network thus V1.5 exhibited a slightly higher elongation at break (ε_{break} = 637 ± 127 %) than V1 (ε_{break} = 596 ± 95 %).

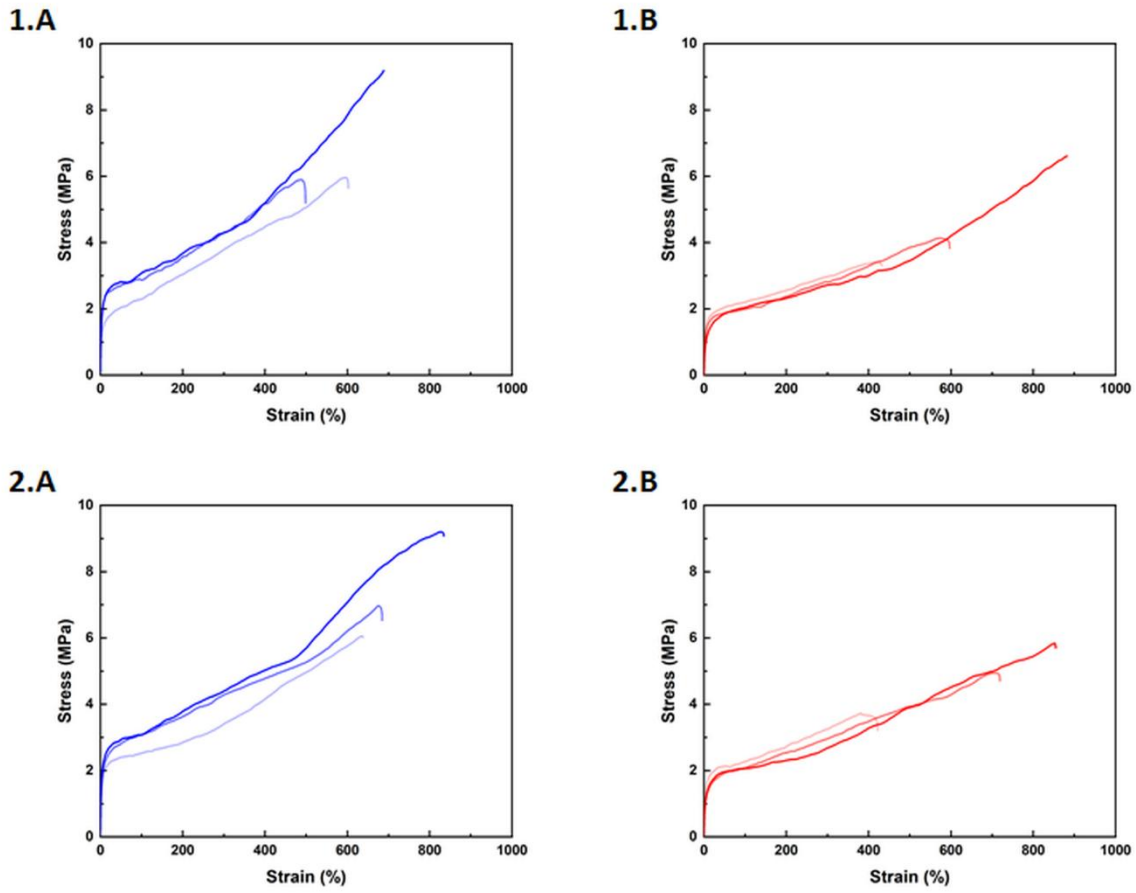

Figure 3. Stress-strain tensile curves for V1 (A) and V1.5 (B): 1. after crosslinking, and 2. after 3 reshapings.

3.3. Network dynamics

To highlight the dynamics of the networks, the viscoelastic properties of the imine vitrimers V1 and V1.5 were investigated *via* stress relaxation and creep-recovery experiments. Stress relaxation tests were performed from 60 °C to 85 °C to ensure that the network relaxation induced by the glassy/rubbery state transition occurring at Tg = 20 °C for V1 and at 16 °C for V1.5 was not impacting the phenomenon. The evolution of the relaxation modulus over time is presented in Figure 4. For both networks, fast stress relaxation was observed in the temperature range studied. Indeed, materials were able to relax more than 90 % of the initial storage modulus in less than 100 s, even at moderate temperature. However, the relaxation could not be fitted with Maxwell model even in its stretch version ($G/G_0 = \exp(-t/\tau)^{\beta}$). Indeed, the materials started to relax before actual data can be collected (< 1 s) and only a part of the relaxation was observed. Therefore, the relaxation curves could not be related to a specific relaxation time (τ). This issue has been overviewed in several articles[49,51,52] reporting vitrimers based on imine exchange, hence flow activation energy determined from these inaccurate relaxation time can hardly be considered. In such cases of fast exchange reaction, it is advised to couple the relaxation analyses with other rheological techniques to more accurately characterize the materials.[53]

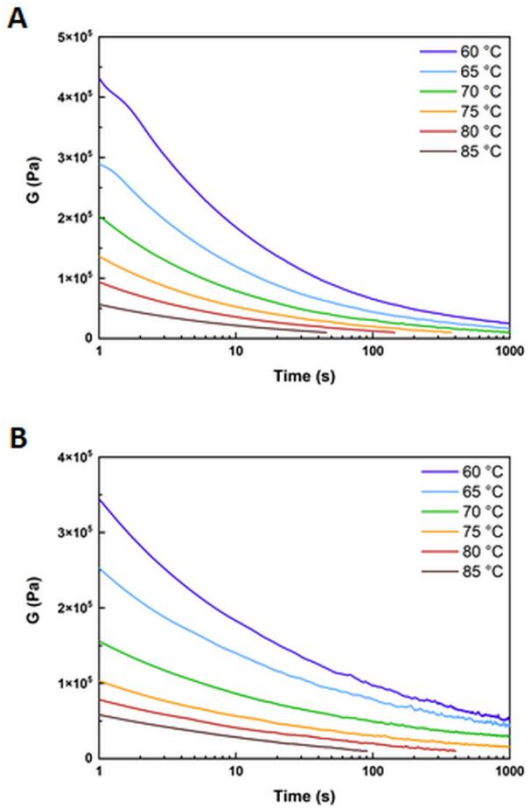

Figure 4. Evolution of relaxation modulus over time at different temperature ranging between 60 and 85°C for hybrid vitrimers V1 (A) and V1.5 (B).

Hence, creep-recovery measurements were performed for temperatures ranging from 60 °C to 85 °C. A constant stress of 500 Pa was applied on the sample for 30 min followed by a recovery time of 30 min and the variation of deformation was followed as a function of time. Creep and recovery results are presented in Figure 5. Both materials were highly stable at the lowest temperature tested (60 °C): only relatively small deformation was observed after 30 min under stress. However, when a sufficient thermal stimulus was applied the dynamics generated by the imine exchange was observed. Indeed, creep tests highlighted an initial elastic deformation corresponding to the chain mobility followed by a plastic deformation due to the reorganisation of the networks enabled by the imine exchange. During recovery, the initial elastic deformation could be recovered whereas the deformation allowed by the imine exchange remained. In the plastic deformation region, the compliance ($J_t = \gamma_t/\sigma$) is supposed to follow a linear law with time and the linear coefficient corresponds to the zero-shear viscosity ($J_t = t/\eta_0 + J_0$). Hence, performing creep experiments at different temperatures allowed η_0 to be determined as a

function of temperature. These creep-recovery experiments showed that η_0 followed an Arrhenius law for both materials with flow activation energy of 137 and 134 kJ.mol^{-1} for V1 and V1.5, respectively (Figure 6). Despite their structural differences, the flow activation energies of the two materials were almost identical. A lower activation energy for V1.5 was expected as its crosslinking density was lower than that of V1.[54–56] However, these two materials were not based exactly on the same exchange reactions. Theoretically, V1 was only based on imine metathesis as no free amines were present in the network, whereas in V1.5 transimination could occur concomitantly with imine metathesis due to the presence of the free amines in the network. Consequently, the flow activation energies could hardly be compared as there is no clear trend on whether the combination of two exchange reactions increases or decreases these energies.[57–59] Regarding the viscosity, V1 displayed a higher value than V1.5 in the range of temperature studied indicating that relaxation is slightly faster in V1.5 than in V1 as relaxation time and viscosity are proportional.[53] This result may be explained by the lower crosslinking density of V1.5 compared to V1 which facilitates the imine exchange.

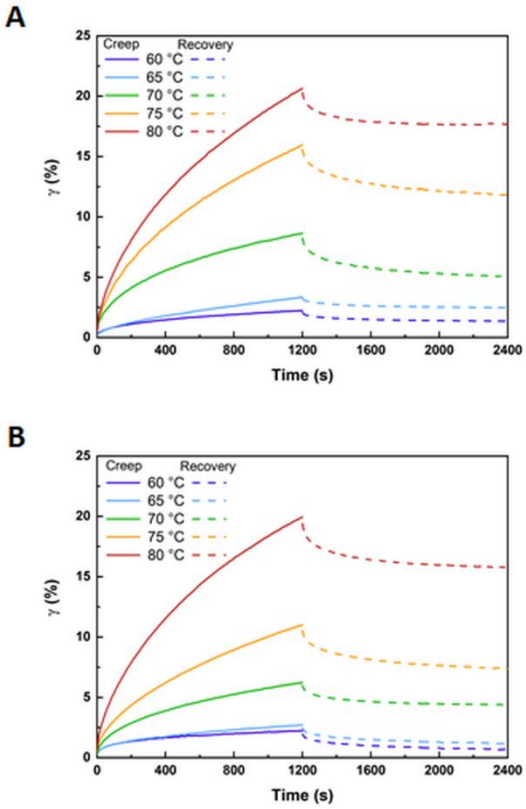

Figure 5. Creep (500 Pa) and recovery experiments in the 60-85°C range of hybrid vitrimers V1 (A) and V1.5 (B).

These rheological experiments enabled to highlight the dynamic character of these two networks and demonstrated how by tuning the structure of the network, the characteristic properties of imine vitrimers could be impacted. The fast exchange rate observed for these two vitrimer materials based on imine exchange should enable easy reprocessing.

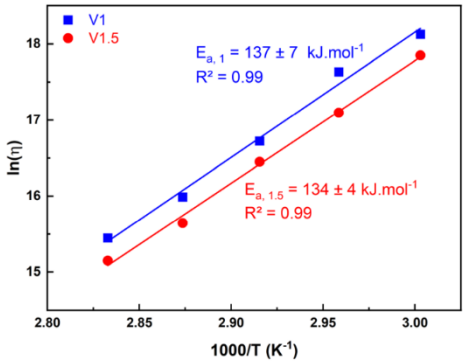

Figure 6. Arrhenius plot for hybrid vitrimers V1(blue squares) and V1.5 (red circles).

3.4. Reprocessing and self-healing

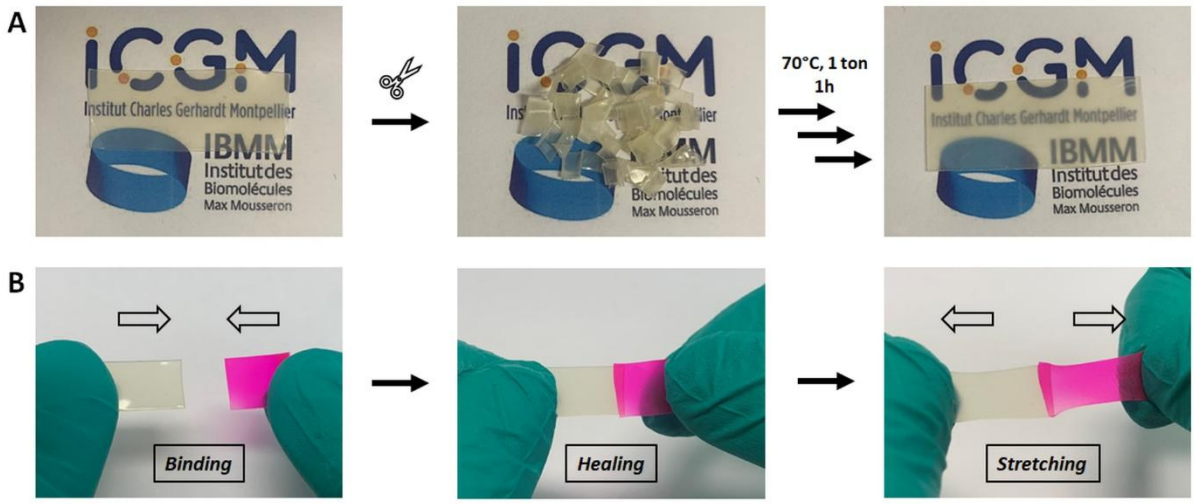

Figure 7. (A) Visual aspect of V1.5 before (left) and after (right) reshaping. The middle picture shows the fragments of V1.5 before reshaping. (B) Self-healing evaluated by visual recovery.

Rheological experiments demonstrated the dynamic character of imine exchange capable networks V1 and V1.5. The recyclability of imine vitrimers was assessed by performing a series of reprocessing tests and characterizing the reprocessed materials. After optimization, visually satisfactory results were

obtained by treating the materials at 70 °C for 1 h under 1 t (Figure 7). The temperature was maintained under 100 °C to ensure that no undesirable amide would form. Indeed, above 100 °C the amidation of the ester functions constituting the PLA chains could occur.[60] The temperature chosen was also below the 5 % weight degradation temperature of the samples, thus preventing potential material degradation during reprocessing. To confirm the good reprocessing of the materials under these conditions, the properties of the materials reprocessed 3 times were compared to those of the initial networks. Gel fraction measurements indicated that the reshaping process had no apparent impact on the crosslinking density of the materials since values of 85 and 82 %, similar to the original ones, were obtained for V1 and V1.5, respectively. DSC thermograms (Figure S10) exhibited identical glass transition temperatures before and after reprocessing; and similar TGA thermograms showed that thermal stability was retained after reprocessing (Figure S8). In addition, FTIR (Figure S11) and TGA (Figure S8) confirmed that the structure of the material was not modified by the reprocessing steps. Finally, the mechanical properties of the 3 times reshaped samples were evaluated via tensile tests. As displayed in Table 2, the designed materials could be reshaped 3 times without impacting their mechanical properties. Indeed, the strain-stress curves showed similar behaviours to the initial ones. Moreover, the values of mechanical properties were equal to the original ones.

In addition to the reprocessing properties, the self-healing capability of the networks was assessed visually (Figure 7). Two pieces of pristine materials were able to bind and form a single new material after having been placed in contact at 70 °C for 1 h. This self-healing property is of high interest for the development of biomedical applications.[28] For instance, the biomaterial would be able to heal after damages caused by user manipulation or after positioning by a surgeon.

3.5. Degradability study

The degradation of the materials was studied by monitoring the mass loss when immersed in PBS (pH 7.4) at 37°C (Figure 8). The two networks displayed similar behaviours with a linear degradation profile and a remaining mass of 84 ± 1 % for V1 and 86 ± 1 % for V1.5 after 46 days. These results showing a slow hydrolytic degradation are in agreement with the large amount of hydrophobic PLA units in the network backbone, as well as the presence of chemical crosslinks. Moreover, the two

systems exhibited similar properties due to their very close chemical composition. These results confirm that the networks can be further envisioned for the development of temporary degradable medical devices.

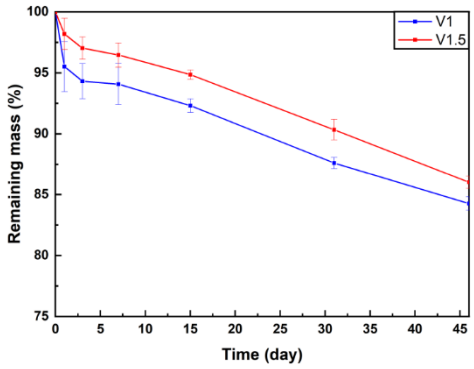

Figure 8. Evaluation of hybrid vitrimers degradation in PBS (pH 7.4) at 37°C.

CONCLUSION

In this work, vitrimers based on dynamic imine exchange were prepared from aldehyde functional di-hydroxyurethane modifier and amine functional 8-arm star PEG-PLA block copolymer. Two materials V1 and V1.5 using initial aldehyde/amine ratio of 1:1 and 1:1.5 were synthesized. Highly crosslinked networks with gel fractions above 82% were obtained thanks to the multi-functionality of the PEG-PLA prepolymer and the hydroxyurethane modifier. As expected, the aldehyde/amine ratio impacted the properties of the materials. Due to the presence of free amines in the network, V1.5 displayed a slightly lower crosslinking density, which resulted in a higher strain and a lower stress at break (ε_{break} = 637 %; σ_{break} = 4.6 MPa) compared to V1 (ε_{break} = 596 %, σ_{break} = 6.7 MPa). For both networks, fast stress relaxation was observed, which confirmed the dynamic nature of the networks. Moreover, creep-recovery experiments showed that the materials followed an Arrhenius behaviour confirming their vitrimer nature and enabled to estimate the influence of the temperature on the material viscosity. Finally, the samples could be reprocessed thrice without any significant impact on their chemical integrity, mechanical and thermal properties. Overall these results demonstrate that the materials

developed in this study could open the way towards the design of on-demand degradable medical devices, which could be shaped to a desired form under mild conditions using a suitable mold.

Declaration of competing interest

The authors declare that they have no known competing financial interests or personal relationships that could have appeared to influence the work reported in this paper.

Acknowledgements

This work was supported by the ANR2019-OPENN (ANR-19-CE19-0022-02) and the ANR2019-AFCAN (ANR-19-CE06-0014).

Supplementary data

Supplementary data are available online.

References

(1) Tidwell, T. T. Hugo (Ugo) Schiff, Schiff Bases, and a Century of β-Lactam Synthesis. *Angew. Chemie Int. Ed.* **2008**, *47* (6), 1016–1020. https://doi.org/10.1002/anie.200702965.

(2) Vigato, P. A.; Tamburini, S. The Challenge of Cyclic and Acyclic Schiff Bases and Related Derivatives. *Coord. Chem. Rev.* **2004**, *248* (17–20), 1717–2128. https://doi.org/10.1016/j.cct.2003.09.003.

(3) Murahashi, S.-I. Synthetic Aspects of Metal-Catalyzed Oxidations of Amines and Related Reactions. *Angew. Chemie Int. Ed. English* **1995**, *34* (22), 2443–2465. https://doi.org/10.1002/anie.199524431.

(4) Patil, R. D.; Adimurthy, S. Catalytic Methods for Imine Synthesis. *Asian J. Org. Chem.* **2013**, *2*

(9), 726–744. https://doi.org/10.1002/ajoc.201300012.

(5) Meyer, C. D.; Joiner, C. S.; Stoddart, J. F. Template-Directed Synthesis Employing Reversible Imine Bond Formation. *Chem. Soc. Rev.* **2007**, *36* (11), 1705–1723. https://doi.org/10.1039/b513441m.

(6) Belowich, M. E.; Stoddart, J. F. Dynamic Imine Chemistry. *Chem. Soc. Rev.* **2012**, *41* (6), 2003–2024. https://doi.org/10.1039/c2cs15305j.

(7) Liguori, A.; Hakkarainen, M. Designed from Biobased Materials for Recycling: Imine-Based Covalent Adaptable Networks. *Macromol. Rapid Commun.* **2022**, 2100816. https://doi.org/10.1002/MARC.202100816.

(8) Taynton, P.; Yu, K.; Shoemaker, R. K.; Jin, Y.; Qi, H. J.; Zhang, W. Heat- or Water-Driven Malleability in a Highly Recyclable Covalent Network Polymer. *Adv. Mater.* **2014**, *26* (23), 3938–3942. https://doi.org/10.1002/adma.201400317.

(9) Ciaccia, M.; Cacciapaglia, R.; Mencarelli, P.; Mandolini, L.; Di Stefano, S. Fast Transimination in Organic Solvents in the Absence of Proton and Metal Catalysts. A Key to Imine Metathesis Catalyzed by Primary Amines under Mild Conditions. *Chem. Sci.* **2013**, *4* (5), 2253. https://doi.org/10.1039/c3sc50277e.

(10) Ciaccia, M.; Di Stefano, S. Mechanisms of Imine Exchange Reactions in Organic Solvents. *Org. Biomol. Chem.* **2015**, *13* (3), 646–654. https://doi.org/10.1039/C4OB02110J.

(11) Kovaříček, P.; Lehn, J. M. Merging Constitutional and Motional Covalent Dynamics in Reversible Imine Formation and Exchange Processes. *J. Am. Chem. Soc.* **2012**, *134* (22), 9446–9455. https://doi.org/10.1021/ja302793c.

(12) Zhang, Y.; Tao, L.; Li, S.; Wei, Y. Synthesis of Multiresponsive and Dynamic Chitosan-Based Hydrogels for Controlled Release of Bioactive Molecules. *Biomacromolecules* **2011**, *12* (8), 2894–2901. https://doi.org/10.1021/bm200423f.

(13) Kathan, M.; Kovaříček, P.; Jurissek, C.; Senf, A.; Dallmann, A.; Thünemann, A. F.; Hecht, S.

Control of Imine Exchange Kinetics with Photoswitches to Modulate Self-Healing in Polysiloxane Networks by Light Illumination. *Angew. Chemie - Int. Ed.* **2016**, *55* (44), 13882–13886. https://doi.org/10.1002/anie.201605311.

(14) Cuminet, F.; Caillol, S.; Dantras, É.; Leclerc, É.; Ladmiral, V. Neighboring Group Participation and Internal Catalysis Effects on Exchangeable Covalent Bonds: Application to the Thriving Field of Vitrimer Chemistry. *Macromolecules* **2021**, *54* (9), 3927–3961. https://doi.org/10.1021/acs.macromol.0c02706.

(15) Chakma, P.; Konkolewicz, D. Dynamic Covalent Bonds in Polymeric Materials. *Angew. Chemie* **2019**, *131* (29), 9784–9797. https://doi.org/10.1002/ange.201813525.

(16) Wanasinghe, S. V.; Dodo, O. J.; Konkolewicz, D. Dynamic Bonds: Adaptable Timescales for Responsive Materials. *Angew. Chemie Int. Ed.* **2022**. https://doi.org/10.1002/anie.202206938.

(17) Denissen, W.; Winne, J. M.; Du Prez, F. E. Vitrimers: Permanent Organic Networks with Glass-like Fluidity. *Chem. Sci.* **2016**, *7* (1), 30–38. https://doi.org/10.1039/C5SC02223A.

(18) Zheng, N.; Xu, Y.; Zhao, Q.; Xie, T. Dynamic Covalent Polymer Networks: A Molecular Platform for Designing Functions beyond Chemical Recycling and Self-Healing. *Chem. Rev.* **2021**, *121* (3), 1716–1745. https://doi.org/10.1021/acs.chemrev.0c00938.

(19) Jin, Y.; Lei, Z.; Taynton, P.; Huang, S.; Zhang, W. Malleable and Recyclable Thermosets: The Next Generation of Plastics. *Matter* **2019**, *1* (6), 1456–1493. https://doi.org/10.1016/j.matt.2019.09.004.

(20) Memon, H.; Liu, H.; Rashid, M. A.; Chen, L.; Jiang, Q.; Zhang, L.; Wei, Y.; Liu, W.; Qiu, Y. Vanillin-Based Epoxy Vitrimer with High Performance and Closed-Loop Recyclability. *Macromolecules* **2020**, *53* (2), 621–630. https://doi.org/10.1021/acs.macromol.9b02006.

(21) Geng, H.; Wang, Y.; Yu, Q.; Gu, S.; Zhou, Y.; Xu, W.; Zhang, X.; Ye, D. Vanillin-Based Polyschiff Vitrimers: Reprocessability and Chemical Recyclability. *ACS Sustain. Chem. Eng.* **2018**, *6* (11), 15463–15470. https://doi.org/10.1021/acssuschemeng.8b03925.

(22) Huang, K.; Ma, S.; Wang, S.; Li, Q.; Wu, Z.; Liu, J.; Liu, R.; Zhu, J. Sustainable Valorization of Lignin with Levulinic Acid and Its Application in Polyimine Thermosets. *Green Chem.* **2019**, *21* (18), 4964–4970. https://doi.org/10.1039/c9gc02384d.

(23) Fu, B.; Cheng, B.; Jin, X.; Bao, X.; Wang, Z.; Hu, Q. Chitosan-Based Double Network Hydrogels with Self-Healing and Dual-Responsive Shape Memory Abilities. *J. Appl. Polym. Sci.* **2019**, *136* (47), 48247. https://doi.org/10.1002/app.48247.

(24) Ding, F.; Wu, S.; Wang, S.; Xiong, Y.; Li, Y.; Li, B.; Deng, H.; Du, Y.; Xiao, L.; Shi, X. A Dynamic and Self-Crosslinked Polysaccharide Hydrogel with Autonomous Self-Healing Ability. *Soft Matter* **2015**, *11* (20), 3971–3976. https://doi.org/10.1039/c5sm00587f.

(25) Lin, S. H.; Papadakis, C. M.; Kang, J. J.; Lin, J. M.; Hsu, S. H. Injectable Phenolic-Chitosan Self-Healing Hydrogel with Hierarchical Micelle Architectures and Fast Adhesiveness. *Chem. Mater.* **2021**, *33* (11), 3945–3958. https://doi.org/10.1021/acs.chemmater.1c00028.

(26) Khan, M.; Koivisto, J. T.; Hukka, T. I.; Hokka, M.; Kellomäki, M. Composite Hydrogels Using Bioinspired Approach with in Situ Fast Gelation and Self-Healing Ability as Future Injectable Biomaterial. *ACS Appl. Mater. Interfaces* **2018**, *10* (14), 11950–11960. https://doi.org/10.1021/acsami.8b01351.

(27) Lü, S.; Gao, C.; Xu, X.; Bai, X.; Duan, H.; Gao, N.; Feng, C.; Xiong, Y.; Liu, M. Injectable and Self-Healing Carbohydrate-Based Hydrogel for Cell Encapsulation. *ACS Appl. Mater. Interfaces* **2015**, *7* (23), 13029–13037. https://doi.org/10.1021/acsami.5b03143.

(28) Grosjean, M.; Gangolphe, L.; Nottelet, B. Degradable Self- healable Networks for Use in Biomedical Applications. *Adv. Funct. Mater.* **2023**, 2205315. https://doi.org/10.1002/adfm.202205315.

(29) Bello, D.; Woskie, S. R.; Streicher, R. P.; Liu, Y.; Stowe, M. H.; Eisen, E. A.; Ellenbecker, M. J.; Sparer, J.; Youngs, F.; Cullen, M. R.; Redlich, C. A. Polyisocyanates in Occupational Environments: A Critical Review of Exposure Limits and Metrics. *Am. J. Ind. Med.* **2004**, *46*

(5), 480–491. https://doi.org/10.1002/ajim.20076.

(30) Bello, D.; Herrick, C. A.; Smith, T. J.; Woskie, S. R.; Streicher, R. P.; Cullen, M. R.; Liu, Y.; Redlich, C. A. Skin Exposure to Isocyanates: Reasons for Concern. *Environ. Health Perspect.* **2007**, *115* (3), 328–335. https://doi.org/10.1289/ehp.9557.

(31) Ecochard, Y.; Caillol, S. Hybrid Polyhydroxyurethanes: How to Overcome Limitations and Reach Cutting Edge Properties? *Eur. Polym. J.* **2020**, *137*, 109915. https://doi.org/10.1016/j.eurpolymj.2020.109915.

(32) Carré, C.; Ecochard, Y.; Caillol, S.; Avérous, L. From the Synthesis of Biobased Cyclic Carbonate to Polyhydroxyurethanes: A Promising Route towards Renewable Non- Isocyanate Polyurethanes. *ChemSusChem* **2019**, *12* (15), 3410–3430. https://doi.org/10.1002/cssc.201900737.

(33) Nohra, B.; Candy, L.; Blanco, J. F.; Guerin, C.; Raoul, Y.; Mouloungui, Z. From Petrochemical Polyurethanes to Biobased Polyhydroxyurethanes. *Macromolecules* **2013**, *46* (10), 3771–3792. https://doi.org/10.1021/ma400197c.

(34) Blattmann, H.; Fleischer, M.; Bähr, M.; Mülhaupt, R. Isocyanate- and Phosgene-Free Routes to Polyfunctional Cyclic Carbonates and Green Polyurethanes by Fixation of Carbon Dioxide. *Macromol. Rapid Commun.* **2014**, *35* (14), 1238–1254. https://doi.org/10.1002/marc.201400209.

(35) Yadav, N.; Seidi, F.; Crespy, D.; D'Elia, V. Polymers Based on Cyclic Carbonates as Trait d'Union Between Polymer Chemistry and Sustainable CO 2 Utilization. *ChemSusChem* **2019**, *12* (4), 724–754. https://doi.org/10.1002/cssc.201802770.

(36) Bobbink, F. D.; van Muyden, A. P.; Dyson, P. J. En Route to CO 2 -Containing Renewable Materials: Catalytic Synthesis of Polycarbonates and Non-Isocyanate Polyhydroxyurethanes Derived from Cyclic Carbonates. *Chem. Commun.* **2019**, *55* (10), 1360–1373. https://doi.org/10.1039/C8CC07907B.

(37) Blain, M.; Cornille, A.; Boutevin, B.; Auvergne, R.; Benazet, D.; Andrioletti, B.; Caillol, S. Hydrogen Bonds Prevent Obtaining High Molar Mass PHUs. *J. Appl. Polym. Sci.* **2017**, *134* (45), 44958. https://doi.org/10.1002/app.44958.

(38) Besse, V.; Camara, F.; Méchin, F.; Fleury, E.; Caillol, S.; Pascault, J. P.; Boutevin, B. How to Explain Low Molar Masses in PolyHydroxyUrethanes (PHUs). *Eur. Polym. J.* **2015**, *71*, 1–11. https://doi.org/10.1016/j.eurpolymj.2015.07.020.

(39) Birukov, O.; Il, H.; Il, H. Epoxi-Amine Composition Modified with Hydroxyalkyl Urethane, 2010.

(40) Cornille, A.; Auvergne, R.; Figovsky, O.; Boutevin, B.; Caillol, S. A Perspective Approach to Sustainable Routes for Non-Isocyanate Polyurethanes. *Eur. Polym. J.* **2017**, *87*, 535–552. https://doi.org/10.1016/j.eurpolymj.2016.11.027.

(41) Grosjean, M.; Ouedraogo, S.; Déjean, S.; Garric, X.; Luchnikov, V.; Ponche, A.; Mathieu, N.; Anselme, K.; Nottelet, B. Bioresorbable Bilayered Elastomer/Hydrogel Constructs with Gradual Interfaces for the Fast Actuation of Self-Rolling Tubes. *ACS Appl. Mater. Interfaces* **2022**, *14* (38), 43719–43731. https://doi.org/10.1021/acsami.2c11264.

(42) Buwalda, S. J.; Nottelet, B.; Coudane, J. Robust & Thermosensitive Poly(Ethylene Glycol)-Poly(ε-Caprolactone) Star Block Copolymer Hydrogels. *Polym. Degrad. Stab.* **2017**, *137*, 173–183. https://doi.org/10.1016/j.polymdegradstab.2017.01.015.

(43) Burns, A. B.; Register, R. A. Mechanical Properties of Star Block Polymer Thermoplastic Elastomers with Glassy and Crystalline End Blocks. *Macromolecules* **2016**, *49* (24), 9521–9530. https://doi.org/10.1021/acs.macromol.6b02175.

(44) Giuntoli, A.; Keten, S. Tuning Star Architecture to Control Mechanical Properties and Impact Resistance of Polymer Thin Films. *Cell Reports Phys. Sci.* **2021**, *2* (10), 100596. https://doi.org/10.1016/j.xcrp.2021.100596.

(45) Liffland, S.; Hillmyer, M. A. Enhanced Mechanical Properties of Aliphatic Polyester

Thermoplastic Elastomers through Star Block Architectures. *Macromolecules* **2021**, *54* (20), 9327–9340. https://doi.org/10.1021/acs.macromol.1c01357.

(46) Snyder, R. L.; Lidston, C. A. L.; De Hoe, G. X.; Parvulescu, M. J. S.; Hillmyer, M. A.; Coates, G. W. Mechanically Robust and Reprocessable Imine Exchange Networks from Modular Polyester Pre-Polymers. *Polym. Chem.* **2020**, *11* (33), 5346–5355. https://doi.org/10.1039/C9PY01957J.

(47) Kremers, W.; Steele, J. W. A Series of Schiff's Bases and Secondary Amine Derivatives from 3-Formyl-10-Methylphenothiazine. *Can. J. Chem.* **1967**, *45* (7), 745–749. https://doi.org/10.1139/v67-122.

(48) Chao, A.; Negulescu, I.; Zhang, D. Dynamic Covalent Polymer Networks Based on Degenerative Imine Bond Exchange: Tuning the Malleability and Self-Healing Properties by Solvent. *Macromolecules* **2016**, *49* (17), 6277–6284. https://doi.org/10.1021/acs.macromol.6b01443.

(49) Jarach, N.; Dodiuk, H.; Kenig, S.; Naveh, N. Rheology—Composition Relationship of Vitrimers Based on Polyethyleneimine. *J. Appl. Polym. Sci.* **2022**, *139* (28), 52353. https://doi.org/10.1002/app.52353.

(50) Schoustra, S. K.; Groeneveld, T.; Smulders, M. M. J. The Effect of Polarity on the Molecular Exchange Dynamics in Imine-Based Covalent Adaptable Networks. *Polym. Chem.* **2021**, *12* (11), 1635–1642. https://doi.org/10.1039/D0PY01555E.

(51) Schoustra, S. K.; Dijksman, J. A.; Zuilhof, H.; Smulders, M. M. J. Molecular Control over Vitrimer-like Mechanics-Tuneable Dynamic Motifs Based on the Hammett Equation in Polyimine Materials. *Chem. Sci.* **2021**, *12* (1), 293–302. https://doi.org/10.1039/d0sc05458e.

(52) Hakkarainen, M.; Xu, Y.; Odelius, K. Photocurable, Thermally Reprocessable, and Chemically Recyclable Vanillin-Based Imine Thermosets. *ACS Sustain. Chem. Eng.* **2020**, *8* (46), 17272–17279. https://doi.org/10.1021/acssuschemeng.0c06248.

(53) Ricarte, R. G.; Tournilhac, F.; Cloître, M.; Leibler, L. Linear Viscoelasticity and Flow of Self-Assembled Vitrimers: The Case of a Polyethylene/Dioxaborolane System. *Macromolecules* **2020**, *53* (5), 1852–1866. https://doi.org/10.1021/acs.macromol.9b02415.

(54) Breuillac, A.; Kassalias, A.; Nicolaÿ, R. Polybutadiene Vitrimers Based on Dioxaborolane Chemistry and Dual Networks with Static and Dynamic Cross-Links. *Macromolecules* **2019**, *52* (18), 7102–7113. https://doi.org/10.1021/acs.macromol.9b01288.

(55) Gablier, A.; Saed, M. O.; Terentjev, E. M. Rates of Transesterification in Epoxy-Thiol Vitrimers. *Soft Matter* **2020**, *16* (22), 5195–5202. https://doi.org/10.1039/d0sm00742k.

(56) Hayashi, M.; Yano, R.; Takasu, A. Synthesis of Amorphous Low: T g Polyesters with Multiple COOH Side Groups and Their Utilization for Elastomeric Vitrimers Based on Post-Polymerization Cross-Linking. *Polym. Chem.* **2019**, *10* (16), 2047–2056. https://doi.org/10.1039/c9py00293f.

(57) Berne, D.; Quienne, B.; Caillol, S.; Leclerc, E.; Ladmiral, V. Biobased Catalyst-Free Covalent Adaptable Networks Based on CF3-Activated Synergistic Aza-Michael Exchange and Transesterification. *J. Mater. Chem. A* **2022**, *6*, 4883–5230. https://doi.org/10.1039/d2ta05067f.

(58) Berne, D.; Coste, G.; Morales-Cerrada, R.; Boursier, M.; Pinaud, J.; Ladmiral, V.; Caillol, S. Taking Advantage of β-Hydroxy Amine Enhanced Reactivity and Functionality for the Synthesis of Dual Covalent Adaptable Networks. *Polym. Chem.* **2022**, *13* (25), 3806–3814. https://doi.org/10.1039/d2py00274d.

(59) Taplan, C.; Guerre, M.; Du Prez, F. E. Covalent Adaptable Networks Using β-Amino Esters as Thermally Reversible Building Blocks. *J. Am. Chem. Soc.* **2021**, *143* (24), 9140–9150. https://doi.org/10.1021/jacs.1c03316.

(60) Snyder, R. L.; Lidston, C. A. L.; De Hoe, G. X.; Parvulescu, M. J. S.; Hillmyer, M. A.; Coates, G. W. Mechanically Robust and Reprocessable Imine Exchange Networks from Modular

Polyester Pre-Polymers. *Polym. Chem.* **2020**, *11* (33), 5346–5355.

https://doi.org/10.1039/C9PY01957J.

For TOC only